PROCEEDINGS, 24th Annual PNOC-EDC Geothermal Conference
Hotel Inter-Continental, Makati City, Philippines, March 12-13, 2003

SCALING AND CORROSION IN SEPARATOR VESSEL 303, BACMAN GEOTHERMAL PRODUCTION FIELD, PHILIPPINES

Sylvia G. Ramos[1], Josephine B. Rosell[1], Keith Lichti[2], Fidel S. See[1], Jimmy J. Fragata[1], Danilo B. Rubin[1], and Raul Evangelista[1]

[1]PNOC Energy Development Corporation, Merritt Road, Fort Bonifacio, Taguig City, Philippines
[2]Materials Performance Technologies, IRL, Lower Hutt, New Zealand

ABSTRACT

Eight scale samples were collected from various parts of Separator Vessel 303 in the Bacman Geothermal Production Field, Philippines during a Risk Based Inspection in December 2001. Gray to black scales having variable thickness up to ~2 mm deposited on the interior walls of the vessel, and on the surface of the steam standpipe. In those instances where thick corrosion products and scales formed, these tended to block the potentially corrosive two-phase and steam fluids from the underlying steel, and minimal corrosion was observed. Areas subject to erosion had thinner corrosion product scales, but corrosion rates were still acceptably low.

Microscopic analysis of scales in the upper part of the separator vessel showed dominance of corrosion products such as magnetite (Fe_3O_4), hematite (Fe_2O_3), pyrrhotite (FeS), and pyrite (FeS_2). SEM EDX analysis confirmed that Fe, S and O are the major components of these scale samples. In the middle and lower portions of the vessel where separated brine is present, scales are made up of amorphous silica (SiO_2) and clay in association with corrosion products. The detection of Si, Al, and Mg by SEM EDX analysis verified the presence of silica and clay in these scale deposits.

The rate of formation of the thin, adherent scales in Separator Vessel 303 is low and hence the scales do not pose any major problem in the operation of the Bacman Fluid Collection and Reinjection System (FCRS). The level of protection provided to the underlying steel by the formed scales is proposed to be dependent on the thickness and adhesion of the formed scales and the self healing characteristics of the scales.

1.0 INTRODUCTION

1.1 Maintenance History

Separator Vessel SV-303 is located at Pad E of BacMan Geothermal Production Field (Fig. 1). It is being used by production wells Pal-12D and Pal-14D to separate the steam from the brine. The steam from these 2 wells passes Steamline-502 towards the pressure reducing station header. It then passes either Steamline-701 or Steamline-702 towards National Power Corporation (NPC) Turbines 1 and 2. The separated brine, along with the separated brine from other separator vessels of Pad-E wells, is then reinjected back in the field through Reinjection Line-722 towards well Pal-1RD.

Vessel SV-303 was first commissioned in 1993. The first Preventive Maintenance Service (PMS) of SV-303 was done in March 1995. The two side vessel manways were both generally clean with a very thin layer (~0.6 mm thick) of white colored silica deposit at the manways. Likewise, the steam standpipe and inner sidewalls were clean except for a rust coloured scale deposit at the crown flange. The next PMS was done in May 1996. At that time the side manway had a dirty white to gray colored brittle and hard silica deposit (~0.8 mm thick). The vessel inner walls and standpipe were also generally clean except for rust coloured particles.

Based on these favorable findings, it was agreed that PMS of SV-303 should be done every two years. Hence, the third PMS was not done until July 1998 while the fourth PMS was in March/April 2001. A fifth and latest PMS was preceded by a Risk Based Inspection completed using procedures developed under a New Zealand Ministry of Foreign Affairs Asia Development Assistance Facility Grant to Materials Performance Technologies and PNOC

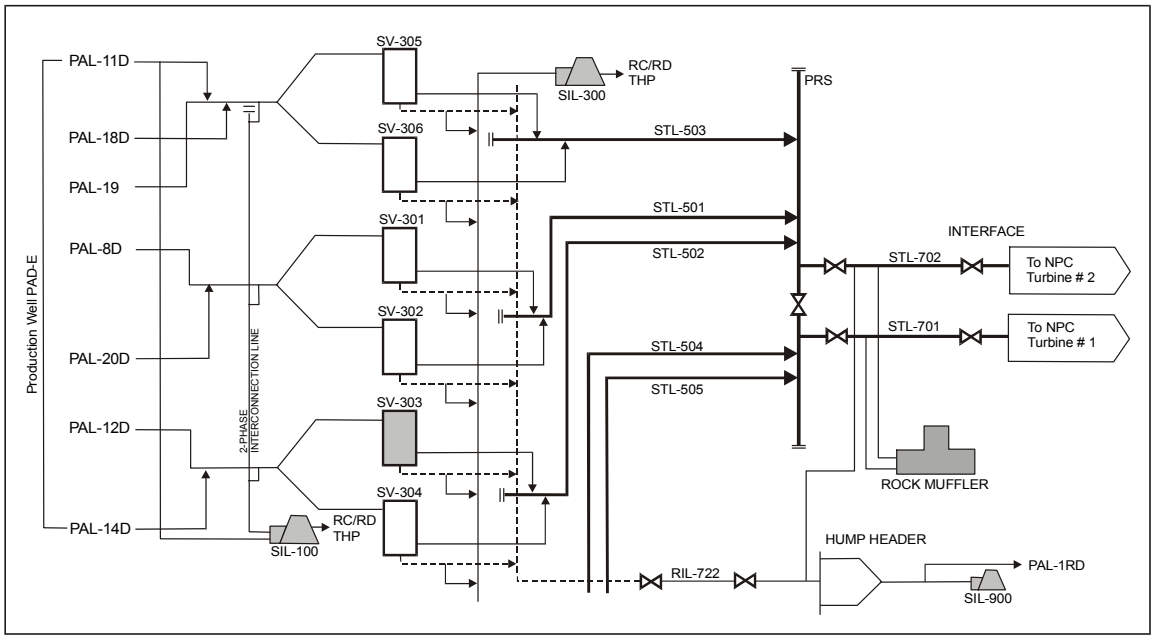

Figure 1. BGPF-1 pad E schematic Fluid Collection and Reinjection System (FCRS).

EDC (Lichti, 2001). The inspection was done in November/December 2001 when the power station was shut down for maintenance activities. This paper describes the results of the Risk Based Inspection.

1.2 Physical/Chemical Environment

SV-303 has been commercially utilized since early 1993. From 1993 to 1995, it was operated using separation pressure of 9 kscg/0.88 MPag (0.98 MPaa/179 deg C). It was then lowered to 8 kscg/0.78 MPag (0.88 MPaa/174.6 deg C) since 1995 to increase steam supply to the power plant.

Table 1 shows the vessel SV-303 material properties and design and fabrication detail.

Chemical analysis results were not available for the steam and water contained within the SV-303 separator vessel and so the chemistry of the two-phase fluid entering and exiting the separator was estimated from the individual well fluid chemistries.

The chemistry of the water phase is dependent on the chemistry and relative amounts of the fluid produced by the 2 wells feeding this separator. The measured chemistries and flow rates were used to predict the Silica Saturation Index for the mixed two-phase fluid (Table 2).

Table 1. Vessel design details of SV-303.

Capacity	400,000 tons per hour
Design Pressure	2.14 Mpag
Operating Pressure	1.00 MPaa (min)/ 1.25 MPaa (max)
Operating Temperature	216 deg C
Hydrotest Pressure	32.2 Mpag
Code	ASME Section VIII Div. I
Date Manufactured	May 1990
Method of Construction	Welding
Material of Construction	A. Shell/Head - A515C-70 B. Skirt Support - A36
General Composition of Vessel Material	Iron: 98.17-97.85% Carbon: 0.33% Manganese: 1.3% Phosphorus: 0.035% Sulfur: 0.035% Silicon: 0.13-0.45%
Non-Destructive Test (NDT)	100% radiography
Post Weld Heat Treatment	Enclose Furnace

The chemistry of separated steam from the individual wells Pal-12D and Pal-14D was used to estimate the high temperature steam condensate chemistry of the individual wells and this was combined to give an estimate of the corrosion chemistry in the upper part of SV-303 (Table 2).

Table 2. Estimated mixed fluid chemistry of water and steam in the SV-303 separator.

Parameter	Estimated	Units
Temperature	175	°C
Pressure	880	KPaa
Water Phase Chemistry		
SiO_2	839	mg/kg
Chloride	6684	mg/kg
SiO_2 Saturation Index	1.09	
Combined Steam Chemistry	(calculated at 175°C)	
Total CO_2 + HCO_3^-	8.88×10^{-4}	mol/kg
Total H_2S + HS^-	7.70×10^{-5}	mol/kg
Total NH_3 + NH_4^+	3.64×10^{-4}	mol/kg
pH_2	0.11	Kpa
pH (175°C)	6.32	
pH (175°C) Neutral	5.72	

Table 3. Location of samples for corrosion product and scale collection and companion locations for ultrasonic thickness measurements of remaining wall thickness.

Scale Collection	Wall Thickness	Location
Sample 1		Top of deflector
Sample 2	Position A	Crown at 3 o'clock
Sample 3	Position B	Below top weld at 3 o'clock
Sample 4	Position D	3.2 m., just below weld
Sample 5		2.5 m. at 3 o'clock
Sample 6		At entry level, 2m. above baffle
Sample 7		Silica slab sample
Sample 8		Outside of standpipe
	Position M	Base of Separator

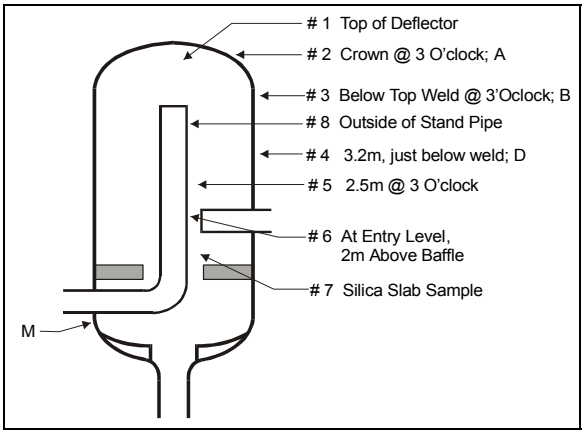

Figure 2. Location of samples and UT measurements in SV-303.

2.0 RISK BASED INSPECTION

2.1 Corrosion Products and Mineral Scales

On November 25, 2001, the side and top manhole of SV-303 were opened for inspection. Gray to black scale deposits of thickness up to ~2 mm were observed on the inside and surface of steam standpipe and inside wall of the vessel. Eight (8) scale samples were then taken from SV-303 during the Risk Based Inspection in December 2001. The samples were collected to help define the scaling and corrosion mechanisms to allow better prediction of the expected performance of the vessel so that an extended period before the next inspection (greater than 2 years) could be justifiably considered.

Sample points for scale and corrosion product collection are given in Table 3 and illustrated in Figure 2.

The samples taken from the top face of the deflector plate (sample 1) consisted of lots of loose corrosion products with multiple layers of apparently crystalline deposits. Sample 2 was taken from crown area above the level of the baffle at the 3 o'clock position. It was composed of pale grey to black small to medium flakes, which easily disintegrated. Sample 3 from below the top weld at 3 o'clock position and yielded brown coloured corrosion products, which were not easily removed from the sidewall. Vigorous scraping with a chisel gave a large number of small chips that were then collected for analysis. The fourth sample was at 3.2 meters, just below one of the circumferential welds. A small amount of fine black powder was collected. In sample #5 (2.5 m above baffle plate at 3 o'clock), the collection was mostly corrosion products, with some silica and dark gray, fine powder. Sample 6 was scraped by a knife from the top of the 2-phase fluid entry level. This sample appeared to be powdery with fine flakes of silica and some corrosion products. Sample 7 is a silica slab speckled with corrosion products on the back side. It was wet and easily dislodged. It shrank by about 50% when dried. The last sample, collected from outside of standpipe inside curvature next to surface, consisted of 2 mm-thick gray, black and brown coloured flakes.

2.2 Ultrasonic Thickness Measurements

The initial visual inspection suggested scale and corrosion product deposition over the majority of exposed surfaces with no obvious areas of localized corrosion. The surfaces were generally smooth in appearance with no significant local growths as might be expected if pitting corrosion were occurring. Of note was the apparent thin corrosion product films in the upper wall area just below the dome to wall weld (Fig. 3).

Ultrasonic thickness measurements were made using a Panametrics Model 36DL meter at a number of locations in the vessel. Table 3 highlights those areas of major interest for this paper, namely the areas at the top, sidewall and lower tangential fluid entry. These results were intended to be compared with design thickness to predict a corrosion rate, or if the thickness was greater than design, the results would give baseline data for comparison with future measurements.

3.0 SAMPLE ANALYSIS AND WALL THICKNESS RESULTS

3.1 Composition of Corrosion Products and Scales

Sample #1. Top face of deflector plate. The sample was composed wholly of corrosion products. Petrological analysis under the reflected light microscope yielded layered sulfides and oxides. The sulfides consist of 50% pyrite and 35% pyrrhotite, while the oxides consisted of 15% magnetite. The pyrite crystals occured either as anhedral to subhedral crystals forming bands with thickness of 0.08-0.28 mm-thick on both sides of magnetite or as anhedral to euhedral cubes or very fine, lathlike crystals floating within or intimately associated with magnetite. Weak hematite coatings were observed in some pyrite grains. Veinlets (~0.02 mm-thick) of fine cubic pyrite grains cut across magnetite. Pyrrhotite, on the other hand, occurs as euhedral, lathlike or very fine crystals within or on edges of pyrite. The magnetite was either thinly banded (0.36-2.0 mm-thick) with pyrite, or as anhedral and euhedral crystals, corroded and pitted fragments floating within pyrite mass. Some magnetite and pyrrhotite laths were leached out leaving ghost outlines within pyrite.

Figure 3. View of inside of separator showing steam stand pipe, upper side wall and dome with seemingly thin corrosion products in the area of the upper side wall below the dome weld.

Sample #2. Crown area above the level of the baffle at the 3 o'clock position. Fine flaky banded hematized corrosion products were removed from the crown area of the separator vessels. These banded corrosion products were composed of 75% pyrite and 25% hematized magnetite. Pyrite normally banded with or coated or lined hematized magnetite. It had an average band thickness of 0.22 mm. It also occured as fine anhedral to euhedral cubes floating within hematized magnetite. The occurrence of magnetite in this sample was similar to that in Sample # 1. Its band thickness ranged from 0.08-0.2 mm. It also occured as "islands" within or coated by pyrite. Some anhedral to euhedral magnetite laths embedded in pyrite were also leached out.

SEM EDX analysis on this sample yielded major sulfur and iron and minor oxygen. Figure 4 shows SEM view of crystals of iron sulfides (FeS_2) .

Sample #3. Below top weld at 3 o'clock position. Very tiny flakes of corrosion products were collected from this location (Fig. 3). Scanning Electron Microscope (SEM) X-Ray Analysis (EDX) was done on the small samples collected. Figure 5 shows an SEM view of a cross section of metal particle and corrosion product analyzed by SEM EDX as iron and oxygen only. The corrosion product on the sample on the right had iron, sulfur and oxygen while the white area was metallic iron. Another SEM EDX analysis on a cross section of

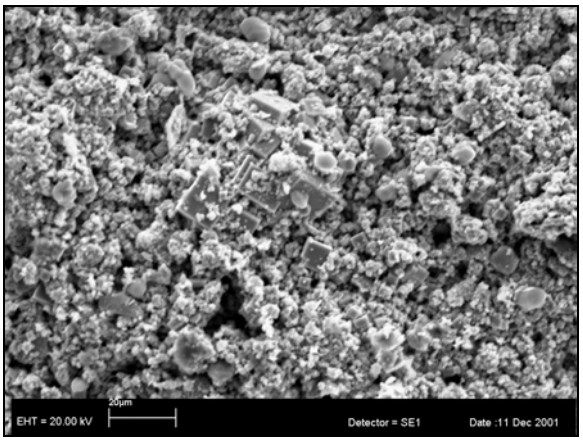

Figure 4. SEM view of top of corrosion product removed as Sample 2, crystals appear to be FeS_2.

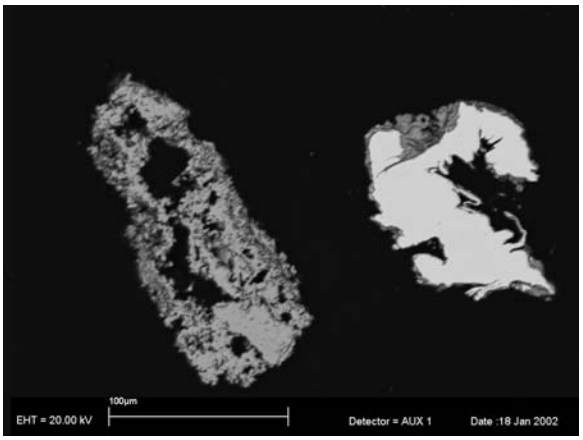

Figure 5. SEM view of cross sections of particles collected as Sample 3, note corrosion product on left contains only Fe/O while white metallic chip on right is Fe with corrosion product containing Fe/O/S.

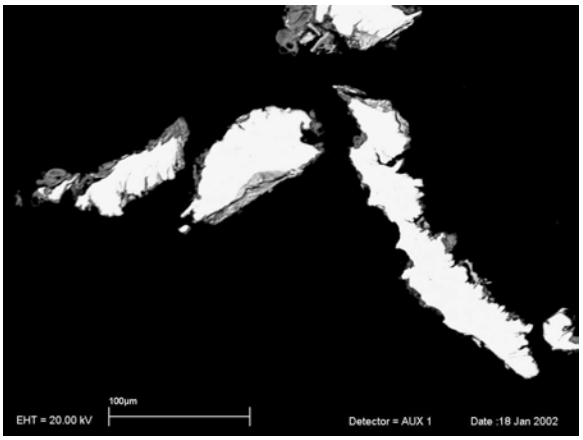

Figure 6. SEM view of metallic flakes of Fe with corrosion products of Fe/O/S and areas not Fe/O.

corrosion products (Fig. 6) yielded mostly iron/oxygen/sulfur and areas of iron/sulfur over metallic iron particles. Figure 6 also shows SEM crosssection view of multilayered metal particles and corrosion products. EDX analysis of this cross section suggests the top layer of corrosion products is mostly magnetite with no sulfur while the lower layer is rich in sulfur, possible pyrite. The middle layer is a mass of iron/oxygen and sulfur, possibly interlayers of magnetite and pyrite.

Sample #4. 3.2 m., just below weld. Small amount of fine black powder collected here consists of ~90% corrosion products and ~10% clay. The corrosion products are made up of 55% hematized magnetite, 25% pyrrhotite and 10% pyrite. The hematized magnetite occurred in pitted layers (partially redissolved) while pyrrhotite was associated with hematized magnetite as fine disseminations, pervasive replacement, stringers (<0.01-0.03mm wide), or finely acicular aggregates. Pyrite appeared as isolated fragments or as stringers (<0.05 mm) in hematized magnetite.

The reddish brown to yellowish clay rims or interlayers with corrosion products.

SEM EDX analysis indicate major components of O, Fe, S, Si, and Al with minor amounts of Mn.

Sample #5. 2.5 m @ 3 o'clock. position. Dark grey, fine powder of mostly corrosion products and probably some silica were collected. Petrologic analysis show the dominance of dark brown, brownish-green to green fibrous clay (63%) which rimmed or interlayered with corrosion products. Minor amount of finely cubic cristobalite (5%) were intimately associated with corrosion products and clay. Corrosion products (30%) consisted of subhedral-anhedral crystalline aggregates or layered hematized magnetite (17%); stringers or disseminations of pyrite (10%) in clay; and pyrrhotite (3%) stringers or as rims in hematized magnetite. Isolated cuttings (2%) were made up of andesite and chalcopyrite.

SEM EDX analysis of the sample show the dominance of O, Fe, Si, Al, and S with minor Mn and Mg.

Sample #6. At entry level, 2 m above baffle. The samples scraped with a knife at the top of two-phase fluid entry level are finely flaky (~1mm) or powdery and are suspected to be silica with some corrosion products. Petrologic analysis showed clear, colorless, layered, occasionally vesicular amorphous silica (40%), clays (38%), corrosion products (20%), and trace chalcopyrite cuttings (2%) embedded in amorphous silica. The clay was green to reddish brown associated with corrosion products or it filled microfractures or vesicles in amorphous silica. The corrosion products were composed of hematized magnetite (10%) and pyrite (10%). Hematized magnetite occurred as anhedral aggregates, stringers, or as fine disseminations (~0.015 mm-0.1 mm) in amorphous silica while pyrite was present as stringers (~0.01 mm wide) and disseminations (<0.01 mm-0.04 mm) in amorphous silica or hematized magnetite.

Sample #7. Silica slab sample. The sample was wet upon collection and was easily dislodged from the wall. It shrank by about 50% upon drying. The front side was grey while the back side was speckled with corrosion products. Petrologic analysis of thin section showed the dominance of clear, colorless, and layered amorphous silica (75%). Occasional shrinkage fracturing was observed. Minor dendritic sphalerite (10%), brown clay laminations or microfracture fills (10%), and corrosion products (5%) were all intimately associated with amorphous silica. The corrosion products were composed of finely (<0.01 mm) disseminated or stringers of chalcopyrite (4%) and pyrite (1%) in amorphous silica; and trace (<1%) inclusion of magnetite in chalcopyrite.

Sample #8. Outside of stand pipe. Thick flakes of gray, black and brown corrosion products were taken from outside of stand pipe, inside curvature next to the surface. The sample yielded multilayered hematized magnetite (60%), pyrrhotite (20%) and 20% pyrite (20%). The hematized magnetite occurred as either thick bands (0.04-0.4 mm thick) with internal concentric layerings, or was locally pitted, finely acicular or globular aggregates. Pyrrhotite minerals were acicular aggregates, anhedral to subhedral rimmings or fine disseminations within hematized magnetite. They also occurred as isolated clusters. Pyrite was seen either as stringers, rimmings or as cubic aggregates within hematized magnetite. Veinlets of cubic pyrite were also observed cutting across hematized magnetite.

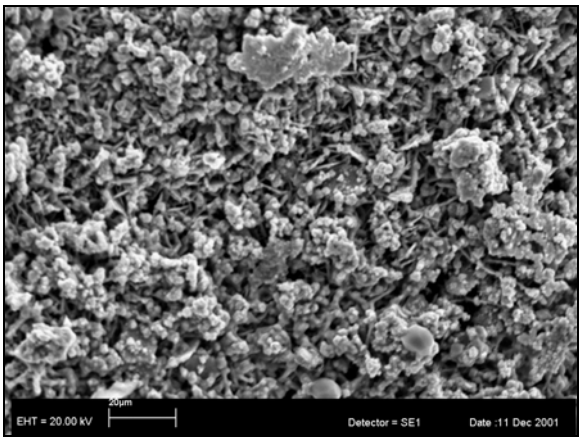

Figure 7. SEM view of inside surface of corrosion products collected from the steam stand pipe.

SEM EDX analysis of crystals from the outside surface indicates the presence of iron sulfides, while analysis of the inside surface suggests iron sulfides and oxygen are present. Figure 7 shows an SEM view of samples from the inside surface of collected product.

3.2 Ultrasonic Thickness results

The results of the Ultrasonic Thickness measurement are given in Table 3. The results show:

- The original thickness of the dome and upper and lower side walls was 20 mm while the central region of the separator wall is thicker at 25 mm.
- The corrosion allowance is 3 mm or greater giving a minimum allowable wall thickness of 17 mm.
- The dome of the vessel is over the design wall thickness of 20 mm (Position A, Sample 2 Location, Fig. 2).
- The wall thickness measurement at the upper side wall (Fig. 3) was the lowest measured but was only 0.67 mm less than original design thickness (Position B, Sample 3, Location, Fig. 2).

- Wall loss in the central and lower areas where corrosion products are formed with entrained clay was low at 0.2 mm (Position D, Sample 4 Location, Fig. 2)

- Wall loss in areas where silica scales were deposited was low (Position M, Fig. 2).

- The exposure time was taken as 8 years assuming the vessel was in more or less continuous service and this gave a maximum corrosion rate of 0.8 mm/year at Position B (Fig. 2)

- Assuming corrosion continues at the same rate, the time to reach the corrosion allowance is 28 years for Position B where thin corrosion product scales form; and 100 to 300 years for areas where thicker corrosion products are formed or silica films deposited.

4.0 SCALING AND CORROSION vs. CORROSION RATES

4.1 Corrosion Products

Corrosion products collected from SV-303 consisted mainly of thin, uniform layers of iron oxides and iron sulfides. These corrosion products were more dominant in the upper portion of the vessel. Textural relationships suggest the intimate association of oxides and sulfides. Iron oxides (magnetite) were formed from electrochemical reactions of iron steel and two-phase fluids entering the vessel. Oxidation of magnetite to hematite is observed in some areas; hematite is also seen altering pyrite in sample #1.

Iron sulfides (pyrrhotite and pyrite) were formed from the reaction of H_2S in steam with Fe steel. Pyrrhotite is usually associated with hematized magnetite as either pervasive replacement or stringers. Pyrite possibly formed later, if not simultaneous, than pyrrhotite. Remnants of pyrrhotite occurred as embedded laths within pyrite layers. Fine cubic pyrite grains were also observed as vein infills cutting the hematized magnetite masses.

The chemistry data of Table 2 was used to prepare a Potential-pH Pourbaix Type diagram for Iron-Water-Sulfur to show the thermodynamic stability of corrosion products in

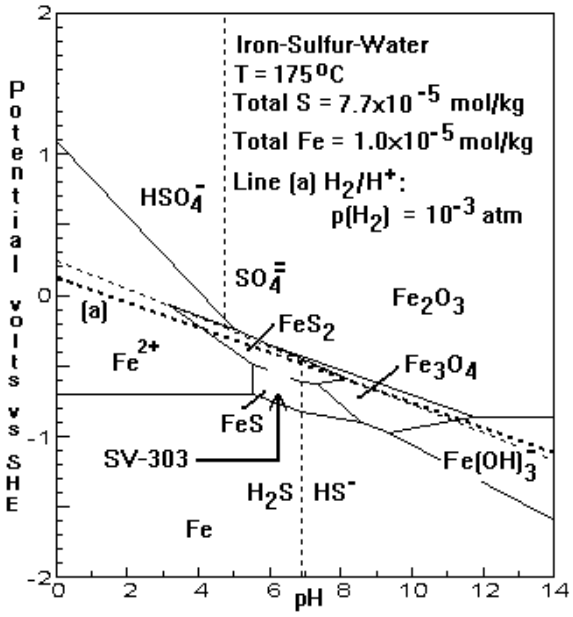

Figure 8. Poubaix diagram for iron-sulfur-water system for BacMan geothermal steam in SV-303 at 175°C.

equilibrium with steam in the upper portion of the separator vessel, Figure 8. Lichti et al. (1997) described the methodology for preparing Pourbaix diagrams and their interpretation for geothermal steam applications. Illustrations of reactions that result in formation of the observed iron sulfide and iron oxide corrosion products include:

$$3Fe + 4H_2O \rightarrow Fe_3O_4 + 8H^+ + 8e$$
$$3Fe^{2+} + 4H_2O \rightarrow Fe_3O_4 + 8H^+ + 8e$$
$$Fe + H_2S \rightarrow FeS + 2H^+ + 2e$$
$$Fe^{2+} + H_2S \rightarrow FeS + 2H^+ + 2e$$
$$Fe^{2+} + 2H_2S \rightarrow FeS_2 + 4H^+ + 2e$$
$$FeS + H_2S \rightarrow FeS_2 + 2H^+ + 2e$$

The previous work has demonstrated that there is a strong tendency to form stable, adherent corrosion products in geothermal steam and that these corrosion products block the underlying metal from the corrosive solution. Pourbaix diagrams of the type shown in Figure 8 describe the stability of these products and the models have been shown to be valid for low chloride, near neutral pH solutions. Based on Figure 8, iron sulfides (pyrite and pyrrhotite) are the corrosion products which are in equilibrium with separated steam at the upper portion of SV 303. The formation of iron sulfide layer reduces concentration of sulfur at the metal surface allowing subsequent deposition of iron oxides.

Below the water level zone, the corrosion products are interlayered with amorphous silica and clays. Fibrous clay layers are also speckled with opaque corrosion products. The corrosion products and scales show a level of intermixing that effectively closes any pores or cracks that form when corrosion products or scales are re-dissolved as a consequence of local chemistry changes or cracked by thermal stresses.

Minor amount of sulfides was collected in the bottom samples where scaling of solids from solution predominates. Chalcopyrite and pyrite stringers and dendritic sphalerite are all intimately associated with amorphous silica and clays, and form from elements transported in solution rather than by corrosion.

4.2 Silica Scaling

Amorphous silica (SiO_2) scales in Samples 6 and 7 were deposited in the vicinity of the entry of the two-phase fluids. It usually rimmed corrosion products suggesting that it was a younger deposit. Another form of silica, cristobalite, was seen as fine crystalline deposits intimately associated with corrosion products and clay in Sample 5.

A silica saturation index (SSI) of 1.09 was predicted for the mixed fluids in SV 303 based on chemistry of wells PAL-12D and PAL-14D, which supply the two-phase fluids to SV-303. The SSI indicates a supersaturation of about 9% giving a reason for the minor silica deposition along the vessel wall where separated brine is present.

4.3 Clay and Dendrite Deposition

Clay scale minerals, dominant in samples 5 and 6, (63% and 38%, respectively), form in the middle portion of the vessel indicating the level of the separated brine in the vessel. It was also present in minor amount (10%) in Samples 4 and 7. The clays occurred in fibrous aggregates as surficial disseminations and laminations in amorphous silica. It rimmed corrosion products, and filled micro fractures, vesicles and other voids in both amorphous silica and corrosion products. These textural relationships suggested that the clay minerals were formed after the corrosion products and amorphous silica were deposited.

The occurrence of corrosion products as “islands” or remnants in a mass of mostly clay and occasional cristobalite (Sample 5) suggests its advanced replacement by clay resulting from the capillary attraction between the separated brine and the solid corrosion products and silica. The clay minerals were also observed as rare micro oolites in Sample 5, appearing in concentric layer with an internal radiating fibrous structure around a nucleus of corrosion product. This texture commonly forms in wave -agitated water which is likely simulated at the surface of the separated brine.

The presence of Si, Al, and Mg, detected by SEM EDX, reflects the composition of the clay scale minerals (silicates) which are most likely iron-bearing swelling clays $(Mg,Fe^{3+}Al)_3[(OH)_2/Al_{>1}Si_{<3}O_{10}].Mg_{0.33}.(H_2O)_4$. The clay scales (silicates) in SV 303 are interpreted to be formed through reaction of silica scales with Al and Mg ions in the brine (Sanchez, pers. comm.), and with Fe in corrosion products. Initially, the silicates are deposited as amorphous masses but with time, these amorphous clays transform to well-crystalline fibers.

The dendrites, mainly composed of sphalerite (ZnS) were apparently deposited directly from the brine on the surface of amorphous silica. The spatial distribution of the dendrites relative to amorphous silica and clay suggests they were deposited after amorphous silica and probably contemporaneous with clay.

4.4 Corrosion Rates

The Ultrasonic Thickness measurements indicate little or no corrosion is occurring in the areas where thick scales are depositing or where dense adherent films of corrosion product are formed in the lower and middle portions of the vessel. In the dome area, the original wall thickness is greater than design and an estimate of corrosion rate cannot be made; however, the appearance suggests an adherent film of corrosion product is present. In the area just below the dome weld on the upper side wall of the vessel, separated steam and steam condensate will be the primary corrodents. The observations made were indicative of the likely damage process:

- The area was a slightly different colour than other areas with thick corrosion products (Fig. 3).
- Scraping yielded minimal corrosion products.
- The chipping activity used to remove material from this area yielded metal pieces with thin layers of corrosion product (Figs. 5 and 6).
- The material lost in this area was greater than in areas where thicker corrosion product films are formed or where silica scales are deposited.

These observations suggest that the metal pieces were standing proud of the surface with thin corrosion product layers over the top. The base material of the surface may also be covered in thin corrosion product. The lack of thick films and roughened metal surface is consistent with the area being subject to erosion-corrosion. This hypothesis is reinforced by the Ultrasonic Thickness measurements that show a readily detectable wall loss of 0.67 mm and suggest an erosion-corrosion rate of 0.08 mm/year (Table 3).

The erosion-corrosion is in part likely due to separator design as the steam must pass from the vessel body into the central standpipe and any steam condensate will tend to be thrown outward to the upper walls in this area. The calculated time to reach the allowed design thickness, i.e., to consume the corrosion allowance, is 28 years for this location and indeed, this is within the design life of the separator but the steam field is expected to have a longer life. The results of the Risk Based Inspection provide early warning of the erosion and allow the area to be targeted for monitoring at future inspections; or for monitoring by external Ultrasonic Thickness measurement either on-line or at scheduled shutdowns. A repair or replace strategy can also be planned well in advance.

In areas where thick corrosion products or adherent silica scales are formed, the remaining lifetimes are in excess of 100 years.

5.0 CONCLUSIONS

Corrosion products composed of magnetite, pyrite, and pyrrhotite are deposited in the upper parts of the SV-303 where separated steam and steam condensate contact the vessel walls. SEM EDX analysis showed a dominance of Fe, O, and S confirming the composition of corrosion products identified by petrological analysis. Regions of high turbulence or high velocity have thinner corrosion product films and show greater material loss suggesting a tendency to erosion-corrosion. For areas subject to erosion-corrosion, the vessel has a predicted remaining life of about 28 years.

In the lower parts of the vessel where separated brine is present, there is a strong tendency to deposition of scales in the form of amorphous silica and clay, together with minor amounts of corrosion products. SEM EDX analysis showed presence of Si, Al, and Mg in samples where silica and clays were observed.

The moderately thick corrosion products and scales in SV 303 are sufficient to block the underlying steel from the corrosive solution, thus resulting in low, acceptable corrosion rates. At the same time, the rate of deposition of scales in SV-303 was sufficiently low so as not to pose major operation concerns with respect to pipe blocking and flow constraints.

An extended operating period before the next shutdown for repeated Risk Based Inspection and PMS is suggested by the initial PMS results and reinforced by this first Risk Based Inspection. Monitoring of operating conditions and chemistry is proposed as a means of ensuring that the physical and chemical conditions remain the same in the interim and that the predicted low scaling rate is maintained. Monitoring of wall thickness by external Ultrasonic Thickness measurement is also recommended to ensure erosion-corrosion rates are within the predicted range.

REFERENCES

Lichti, K. A. (2001). Application of riskbBased inspection methodology to PNOC-EDC geothermal fluid collection and disposal systems: A progress report. *Proceedings, 22nd Annual PNOC-EDC Geothermal Conference, pp. 231-238.*

Lichti, K. A., Wilson, P. T., and Inman, M. E. (1997). Corrosivity of Kawerau geothermal steam. *GRC Transactions, vol. 21, pp 25-32.*